

1
2 **Desulfurization of flue gases using materials**
3 **based on Ca(OH)₂ supported on clays**

4
5 **Roberto Flores^{1*}, Arturo Rodas², David Uscanga², Candi A. Dominguez²**

6 ¹*Universidad Autónoma del Estado de Morelos, Facultad de Ciencias Químicas e Ingeniería,*
7 *Av. Universidad No. 1001, Col. Chamilpa, Cuernavaca, Morelos, 62209, Mexico*

8 ²*Instituto Nacional de Electricidad y Energías Limpias, Calle Reforma 113, Col. Palmira,*
9 *Cuernavaca, Morelos, 62490, Mexico*

10
11
12 **ABSTRACT**

Acid rain is a worldwide environmental problem that started in industrialized countries, and it has been extended to underdeveloped countries. Actions must be taken, and one of those is to deal with one of the major SO₂ emission sources that are thermal power plants. A way of decreasing the SO₂ emissions is to treat the flue gases with sorbent materials, which selectively trap the SO₂. These materials may be based on calcium and many efforts have been recently performed in order to increase their activity and yield. In the present work, SO₂ sorbent materials, based on Ca(OH)₂ at different mass ratios, were prepared supported on clays (bentonite and tonsil), and their activity was tested in a thermogravimetric balance. In addition, ultrasonic energy was applied during preparation trying to improve their performance. It was found that activity increased proportional to the Ca load. Also, when temperature increased from 350 to 450°C, the SO₂ sorption capacity increased. The support clays did not play an important role; at low temperature, activity was slightly better in materials supported on tonsil, but as temperature increased the yield of materials supported on bentonite surpassed those of material supported on tonsil. Ultrasonic energy did not improve the performance of sorbent materials, and, in fact, the sorption capacity diminished when ultrasonic energy was applied during preparation of materials. Finally, the SO₂ sorption process was modeled using a modified shrinking core approach and kinetics parameters were estimated.

13
14 *Keywords: acid rain, Ca(OH)₂, tonsil, bentonite, sorbent materials, flue gas desulfurization,*
15 *ultrasonic energy, kinetics parameter estimation*

16
17
18 **1. INTRODUCTION**

19
20 The combustion of fossil fuel for the generation and/or transformation of energy in sectors,
21 such as, industry, transport and commercial has caused an increase in the concentrations of
22 gaseous and particulate pollutants in the atmosphere. This increase in pollutants has
23 resulted in air pollution. One of the most critical environmental problems is the acid rain,
24 which is a broad term that describes several ways through which acid falls out, including
25 acidic rain, fog, hail and snow. At the beginning of the problem, acidic rainfall was commonly
26 detected around industrial areas; however, with the increased use of tall stacks for power
27 plants and industries, atmospheric emissions are now transported beyond the industrial
28 areas. Acid rain is the result of many steps of chemical reactions between air borne
29 pollutants (oxides of sulfur, nitrogen and other constituents present in the atmosphere) and
30 atmospheric water and oxygen. Main sources of these oxides are fossil fuel fired power
31 stations and smelters for SO₂, and motor vehicle exhausts for NO_x. These oxides may react
32 with other chemicals and produce corrosive substances that are washed out either in wet or
33 dry form by rain as acid deposition [1-3].

34 Acid rain has several effects in the ecosystem, which include the decay in growth of trees,
35 crops, aquatic flora and fauna. In addition, soil fertility is deteriorated as a result of leaching
36 of nutrient cations and the increased availability of toxic heavy metals. Also, stones, metals,
37 paints, textiles and ceramics can be eroded and corroded due to acid rain. It can also
38 indirectly affect human health since it has been shown that SO_2 and NO_x contribute to the
39 formation of $\text{PM}_{2.5}$ [3-6]. The acid rain problem has been tackled to some extent in
40 developed countries by reducing the emission of the precursor gases, and several actions
41 have been created in different parts of the world i.e., the Gothenburg Protocol for the
42 European Union and the US Acid Rain Program in the Title IV of the 1990 Clean Air Act
43 Amendments. [7-10].

44 Due to the rapid economic development and energy consumption throughout the world,
45 fossil fuel consumption has significantly increased during the last few decades. The use of
46 fossil fuel is the major cause of large-scale generation of acid precursors in the atmosphere.
47 The problem was originally identified as an issue in developed countries, but with the
48 increase in industrialization and urbanization, developing countries are now also
49 experiencing this issue.

50 Many reviews have been published related to commercial and pilot-plant technologies for the
51 abatement of SO_2 from thermal power plants [11-13]. Most of the probed technologies are
52 based in calcium sorbents, such as, $\text{Ca}(\text{OH})_2$ and CaO , either in wet or dry conditions. New
53 research efforts have been addressed to improve the yield of calcium materials as SO_2
54 sorbent by mixing it with several supports, such as, silica, fly ash, blast furnace slag, clays,
55 and activated carbon [14-21]. In the present work $\text{Ca}(\text{OH})_2$ was mixed with bentonite and
56 tonsil at many mass ratios. These clays were chosen because they are abundant in Mexico
57 and can be considered a local low-cost raw material, which would reduce the operating cost
58 if they were applied in a local power plant. Bentonite is an aluminiumhydrosilicate, in which
59 the proportion of silicic acid to alumina is about 4:1. On the other hand, tonsil is created from
60 bentonite by acid activation. During this activation, the individual layers are attacked by the
61 acid; as result, aluminum, iron, calcium and magnesium ions are released from the lattice.
62 Also, in a way for further improvement the performance of the sorbent materials, ultrasonic
63 energy may be applied during preparation in an effort to reduce the particle size and
64 increase available active sites as it has occurred in other materials [22-26].

65
66

67 **2. MATERIAL AND METHODS**

68

69 **2.1. Sorbent Preparation**

70 Samples of $\text{Ca}(\text{OH})_2$ supported in bentonite and tonsil were synthesized by preparing
71 slurries at different mass ratio. Some of them were mechanically stirred during 4 h at 60-
72 70°C. In other slurries, ultrasonic energy was applied during 4 h maintaining the temperature
73 below 70°C. After the mixing, slurries were dried overnight a 120°C and pulverized.

74

75 **2.2. Sorbent characterization**

76 To determine the actual calcium content, samples of the sorbent-materials were analyzed by
77 Atomic Absorption Spectroscopy. Table 1 presents the composition of the different materials.

78

79

80

81

82 **Table 1. Calcium composition in the prepared sorbent materials.**

Material	Ca(OH)₂ content [wt%]
Ca-Bentonite 1:2 MS	30.7505
Ca-Tonsil 1:2 MS	34.4440
Ca-Bentonite 1:1 MS	47.7199
Ca-Tonsil 1:1 MS	51.9835
Ca-Bentonite 2:1 MS	67.9053
Ca-Tonsil 2:1 MS	68.0212
Ca-Bentonite 1:2 UE	30.3809
Ca-Tonsil 1:2 UE	32.0253
Ca-Bentonite 1:1 UE	49.7233
Ca-Tonsil 1:1 UE	51.2866
Ca-Bentonite 2:1 UE	64.3171
Ca-Tonsil 2:1 UE	63.6533

83 MS: Mechanical Stirring

84 UE: Ultrasonic Energy

85

86

87 **2.3. Sulfation of sorbents**

88 The sulfation of the materials was carried out in a thermogravimetric balance (TA
89 Instruments 2050) by passing a stream of certified 3600 ppm_v SO₂/N₂ through a known
90 amount of sorbent material. The gas flow rate was 100 mL/min, which is the maximum flow
91 of the thermobalance. The gain of weight in the material was assigned to the sorption of SO₂
92 on the active sites. To ensure reproducibility of the results, the analyzer is monthly calibrated
93 according to international standards by a certified agency.

94

95

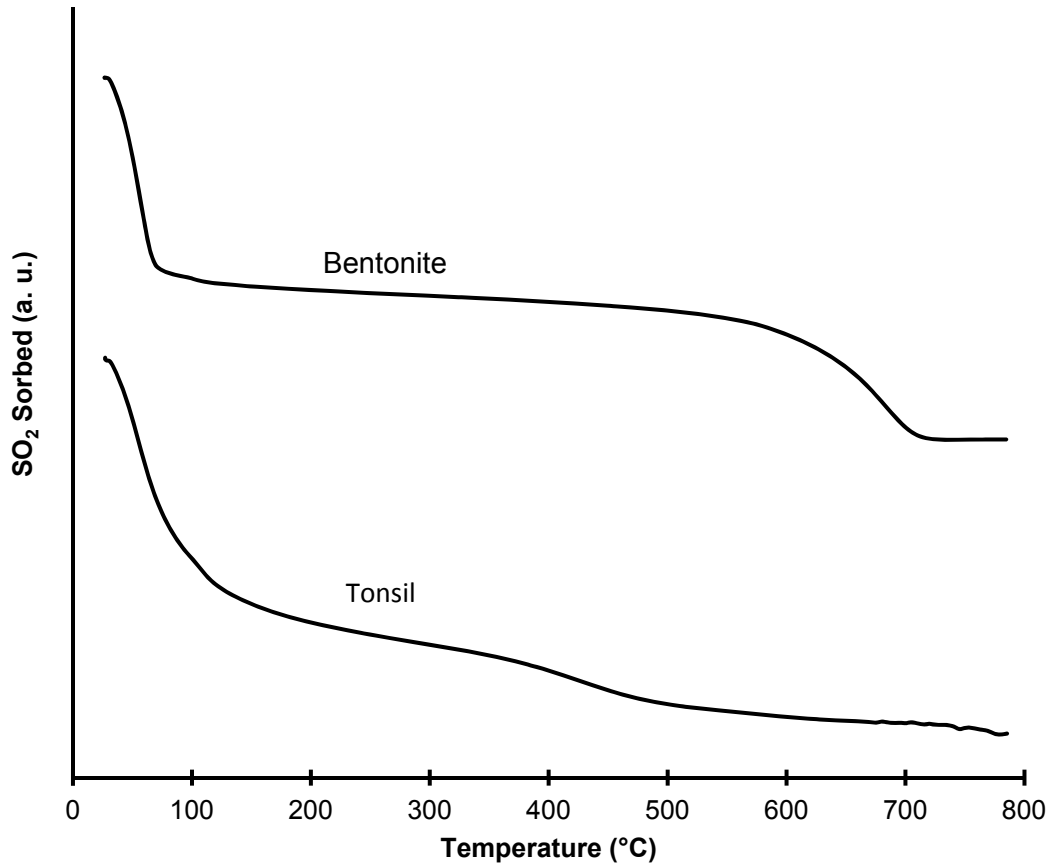
96 **3. RESULTS AND DISCUSSION**

97

98 **3.1. Sorption of SO₂ on bentonite and tonsil**

99 Experiments in the TGA varying temperature (heating rate: 10°C/min) were performed to
100 check if supports were able to adsorb SO₂. Results are presented in Fig. 1, and it was
101 observed that none of the clays retained SO₂. In fact, it was noticed that weight loss
102 occurred as the temperature increased; however, this is attributed to a loss of humidity in the
103 interval between room temperature and 120°C. Then, a drastic weight loss was observed,
104 especially in bentonite, at temperatures higher than 550°C; this is a result of the thermal
105 rearrangement of the crystalline structure.

106

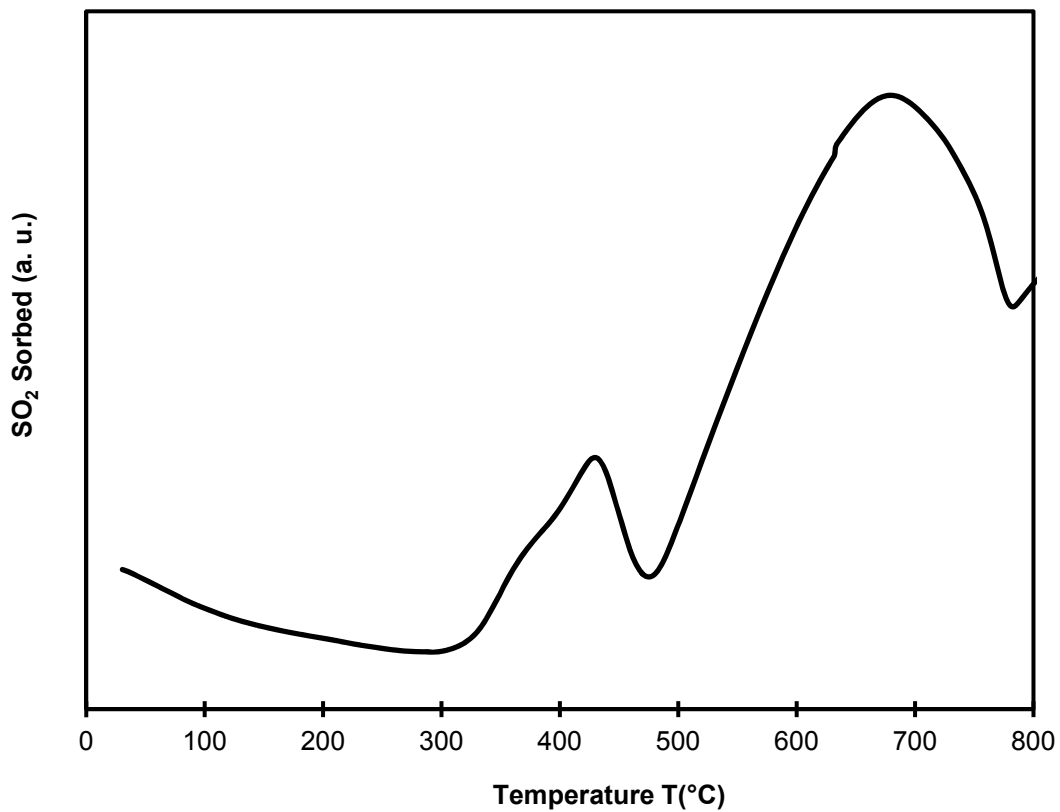


107
 108
 109
 110
 111
 112
 113
 114
 115
 116
 117
 118
 119
 120
 121

Figure 1. Thermogravimetric profiles of the supports in the sulfurization process at variable temperature.

3.2. Effect of temperature in the sorption capacity

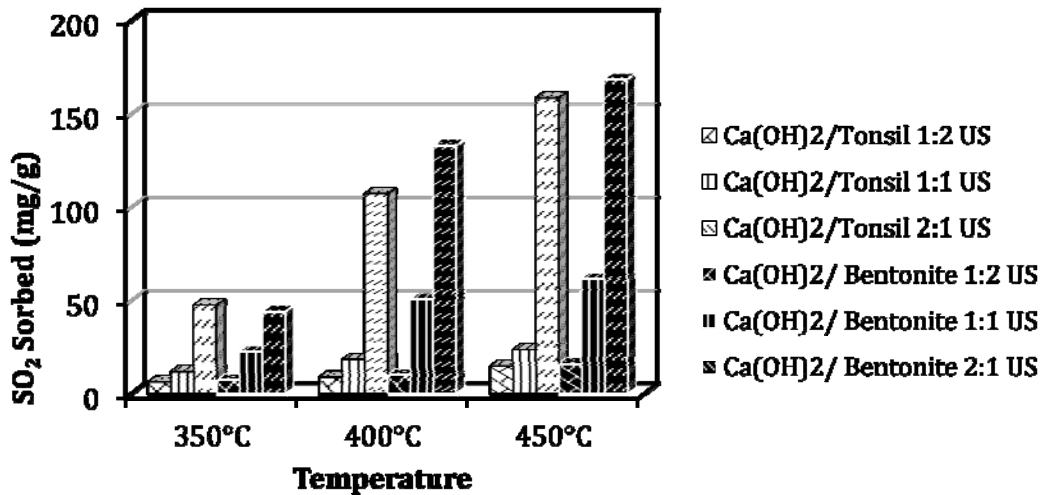
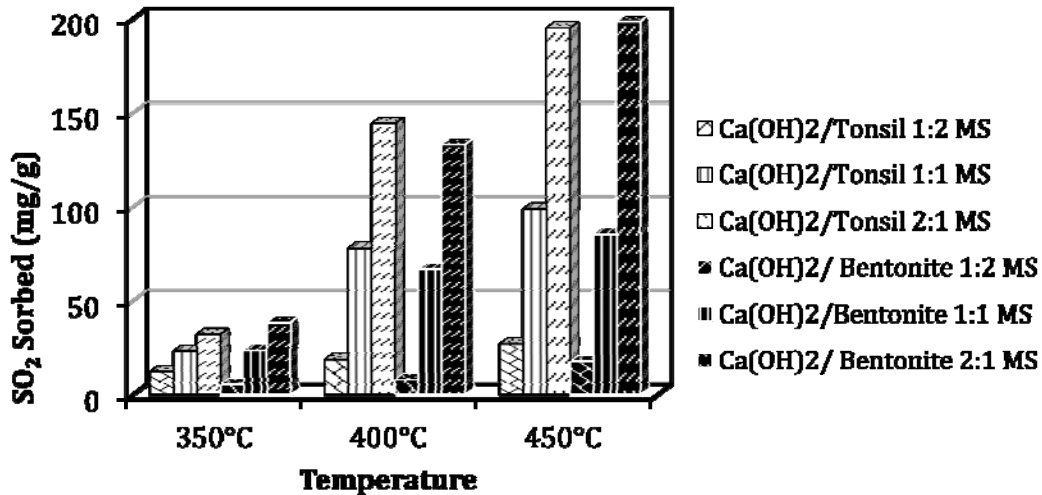
To determine the temperature interval in which the sorbents were studied, an experiment in the TGA with pure Ca(OH)₂ at heating rate of 10°C/min was performed. The result is shown in Fig. 2. It is observed that the SO₂ sorption process begins at 300°C, and it continues up to 650°C. At temperature interval of 420-480°C is noted a drastic loss of weight, but it can be assigned to Ca(OH)₂ decomposition to form CaO, which is also active for adsorbing SO₂. Finally, the selected temperature interval was 350-450°C since at this temperature interval the flue gases enter and exit the preheaters in a thermal power plant, and the proposed technology would be installed at this point.



122
 123
 124
 125
 126
 127
 128
 129
 130

Fig. 2. Thermogravimetric profiles of pure Ca(OH)_2 in the sulfurization process at variable temperature.

Experiments were carried out at constant temperature for 90 min and the amount of SO_2 sorbed in the prepared materials is presented in Fig. 3. It is clearly noticed that as the temperature increases, the sorption capacity of the materials is enhanced. This effect is observed in all materials regardless of the support, Ca load, or preparation method.



131
132
133
134
135
136
137
138
139
140
141
142
143
144
145
146
147
148

Fig. 3. SO₂ sorption capacity of the different prepared materials at 90 min.

3.3. Effect of calcium load

According to the results presented in Fig. 4, Ca load plays an important role in the sorption capacity of the prepared materials as it has been previously reported [Liu et al., 2004; Macias-Perez et al., 2007; Lin et al., 2003]. At lower temperature (350°C) the effect is not well-defined, but as the temperature increases it is observed that Ca load enhances this property. For instance, at 450°C, and considering the material supported on tonsil and prepared with mechanical stirring, at Ca load of 31 wt%, the sorption capacity is 27 mg/g, but as the Ca load increases to 52 wt% (1.7 times), the sorption capacity rises up to 98 mg/g, which is 3.6 times more than at 31 wt %. Moreover, when Ca load is 68 wt% (1.3 times with respect to the last load), the sorption capacity increases 2 times compared to the last load, sorbing 194 mg/g. These results are unexpected; it seems that supports (either tonsil or bentonite) are blocking the active sites instead of providing better dispersion and more active sites. Similar results were previously reported in materials supported on fly ash at low Ca loads [27].

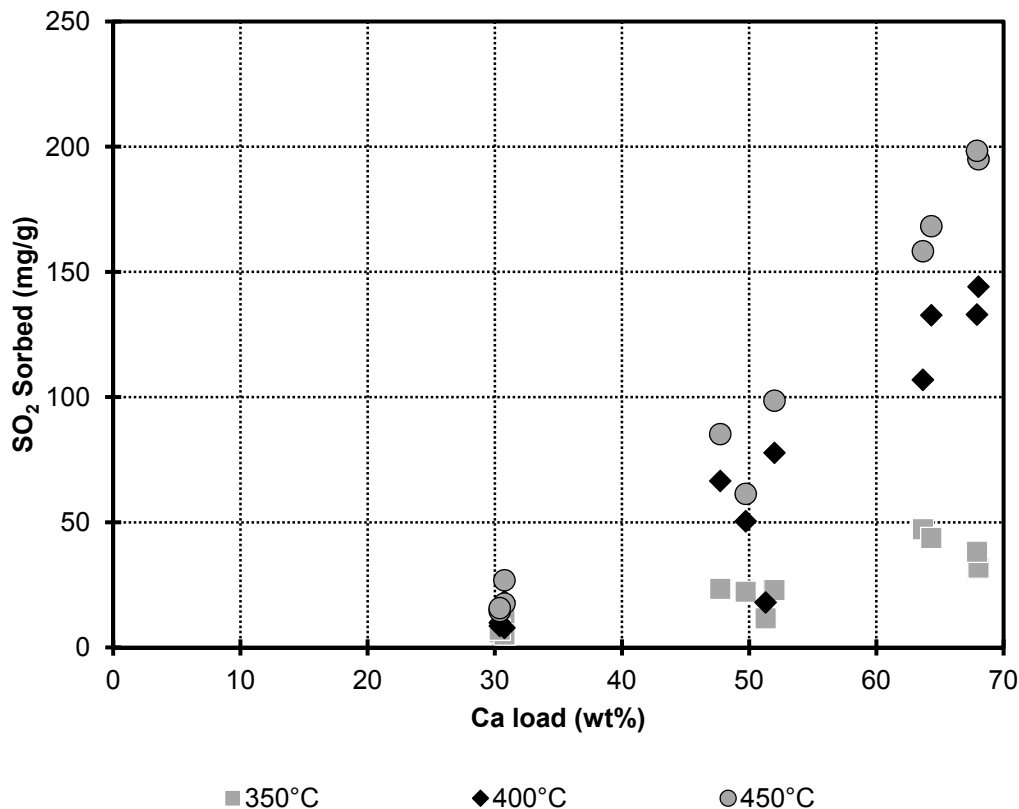


Fig. 4. Effect of calcium load in the SO₂ sorption capacity of the prepared materials.

150
151
152
153

3.4. Effect of support

154
155 The type of support did not show a trend, considering the results presented in Fig. 3. Data
156 suggest that at low Ca loads the materials supported on tonsil result in slightly better yields,
157 but as temperature and Ca load increased this tendency disappears, and finally, at higher
158 temperature (450°C) and Ca load, the better performance was obtained for the material
159 supported on bentonite regardless of preparation method.

160

3.5. Effect of preparation method

161
162 Ultrasonic energy was used trying to improve the yield of the proposed materials. Since the
163 application of ultrasonic materials in slurries is able to fragment the solid particles,
164 decreasing their size, it is proposed that this event would multiply the number of available
165 active sites for the SO₂ sorption process. Nevertheless, the results presented in Fig. 3 do not
166 show an improvement in the performance of the prepared materials. In fact, it is observed
167 that the efficiency of the materials declines when ultrasonic energy is applied during their
168 preparation. This result is attributed to a fusion of the Ca particles when they collide during
169 the application of ultrasonic energy. One of the theories of the particle fragmentation during
170 ultrasonic energy application explains that particles in the slurry are accelerated, and when a
171 collision occurs, they break. Nevertheless, in soft materials, which would be the case of
172 Ca(OH)₂, when the collision happens, the particles are fused, so the particle size increases,
173 and in the case of the present work, would diminish the available active size for the SO₂
174 sorption process.

175
176
177
178
179
180
181
182
183
184
185
186
187
188
189
190
191

3.6. Kinetics parameter estimation

Several models have been developed to represent the heterogeneous non-catalytic solid-gas reaction; however, the most popular used to describe the sulfation of solid sorbents are based on the shrinking core process [28-33]. In this model, it is considered that a first-order chemical reaction between the SO₂ and the calcium core of a spherical particle happens first in the outside surface of the particle forming CaSO₃/CaSO₄. Then, the reaction zone is moved inside the sorbent, leaving behind a converted material and inert solid called “ash” that gradually expands blocking and plugging the pores of the sorbent material because the molar volume of CaSO₃/CaSO₄ is higher than that of CaO or Ca(OH)₂. In this way, there is an inert layer shrinking during the chemical reaction. The relationship between the time and the covered fraction depends on the rate-limiting step. In order for the reaction to proceed, the SO₂ has to diffuse into the new layer, and it has been shown that rate-limiting step for sulfur uptake is the diffusion of SO₂ through the pores of the new product layer on the particle surface [34]. Therefore, the kinetics model that represents the SO₂ sorption process is

$$\frac{t}{k} = \left[3 - 3(1 - \theta)^{2/3} - 2(1 - \theta) \right]$$

$$k = \frac{\rho_B \cdot R^2}{6 \cdot b \cdot D_e \cdot C_g}$$

192 Where: θ is the covered fraction, ρ_B is the molar density of the active sites in the solid, b is
193 the molar ratio of solid reactant to gas reactant (ratio of stoichiometric coefficient), R is the
194 radius of unreacted core, k is the kinetics constant for the surface reaction, C_g is the SO₂
195 concentration in the flue gas, D_e is the effective diffusion coefficient of SO₂ through the “ash”.
196 To improve the adjustment, it was assumed that the SO₂ effective diffusion coefficient, D_e ,
197 depends on the conversion since the new product layer modifies the SO₂ diffusion
198 characteristics through the sorbent material:

$$D_e = D_{e0} \cdot [1 + \alpha_1 e^{(-\alpha_2 \cdot \theta)}]$$

199 Non-linear regression analysis was performed using Polymath™ to determine the kinetics
200 parameters and the results are shown in Tables 2 and 3. According to these results, a good
201 fit was obtained since the R^2_{adj} was high, and with a few exceptions, it was greater than
202 0.99. It is interesting to notice that α_2 takes negative values depending on the calcium load
203 since materials with relationship 1:1 and 2:1 Ca:support, α_2 is negative. This may be
204 assigned to the Ca species formed during sulfation (CaSO₃ or CaSO₄) and their tendency to
205 modify the D_e during the process. A negative α_2 indicates that D_e is not considerable affected
206 by conversion. Fig. 5 and 6 present the fit between the experimental data and the proposed
207 model.

208
209
210
211

Table 2. Kinetics parameters for the SO₂ sorption process in the sorbent materials supported on tonsil.

Material	T [°C]	k [min ⁻¹]	α_1	α_2	R^2_{adj}
Ca-Tonsil 1:2 MS	350	20030	4.304	-13.794	0.9958
	400	7857.592	4.717	-7.582	0.9993
	450	3557.349	11.494	3.899	0.9990
Ca-Tonsil 1:2 UE	350	93860	15.690	49.632	0.9772
	400	25030	22.191	24.597	0.9937
	450	10100	35.430	28.270	0.9897

	350	10360	6.403	-6.203	0.9982
Ca-Tonsil 1:1 MS	400	410.751	1.917	-17.643	0.9981
	450	183.535	0.521	-17.957	0.9983
	350	33790	7.029	-17.333	0.9938
Ca-Tonsil 1:1 UE	400	29330	6.512	8.704	0.9992
	450	11630	8.030	1.545	0.9984
	350	20320	0.167	-69.655	0.9950
Ca-Tonsil 2:1 MS	400	1096.550	4.715×10^{-6}	-56.786	0.9971
	450	637.864	1.357×10^{-8}	-59.974	0.9930
	350	8256.339	0.073	-52.494	0.9967
Ca-Tonsil 2:1 UE	400	2336.802	0.001	-41.779	0.9996
	450	788.094	2.927×10^{-5}	-39.500	0.9694

212
213
214
215
216

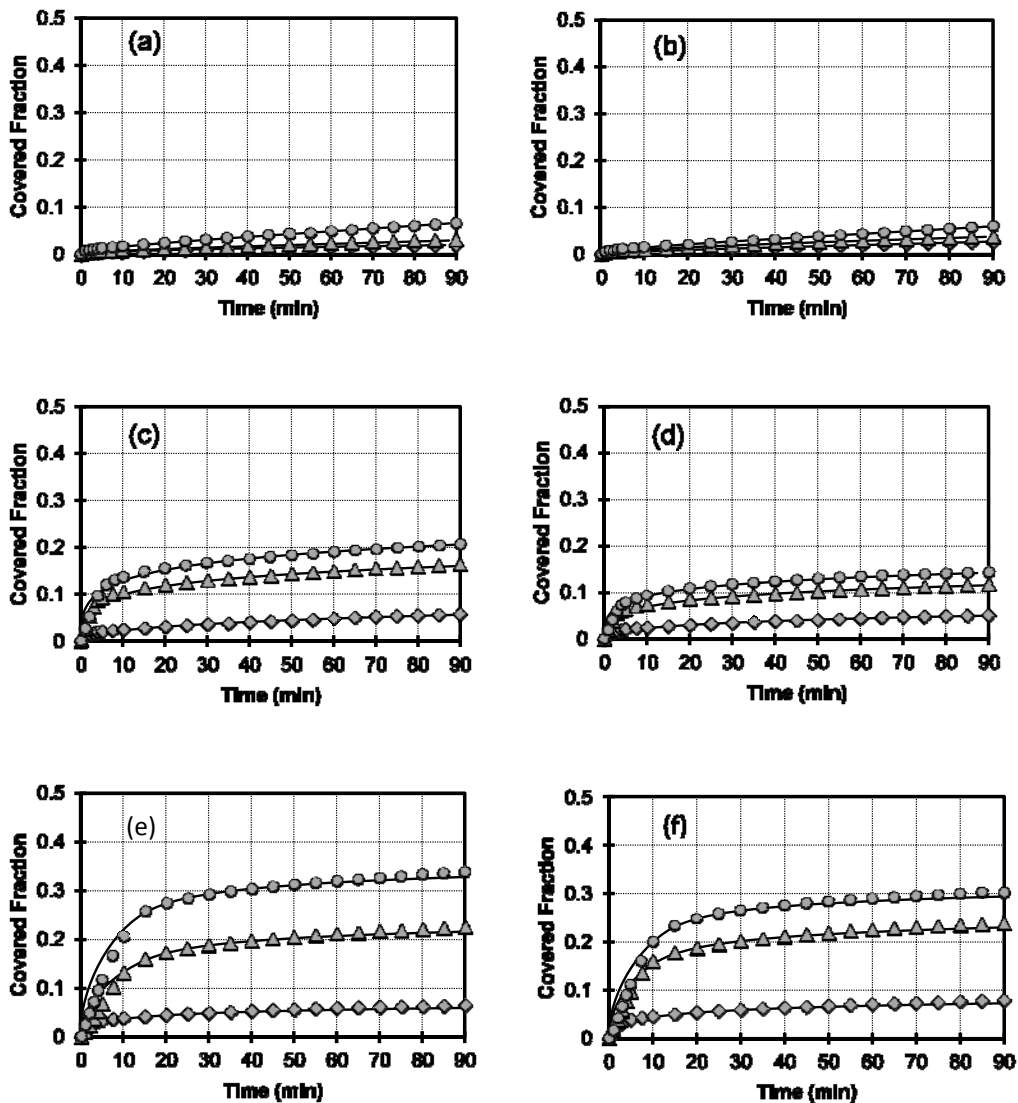
Table 3. Kinetics parameters for the SO₂ sorption process in the sorbent materials supported on bentonite.

Material	T [°C]	k [min ⁻¹]	α_1	α_2	R ² _{adj}
	350	118000	5.989	12.577	0.9961
Ca-Bentonite 1:2 MS	400	43120	13.700	28.002	0.9986
	450	17260	7.5045	16.996	0.9990
	350	159400	5.243	52.851	0.9958
Ca-Bentonite 1:2 UE	400	39910	7.447	19.008	0.9992
	450	14130	11.815	17.397	0.9995
	350	1978.496	22.534	-10.788	0.9987
Ca-Bentonite 1:1 MS	400	170.806	2.150	-20.357	0.9980
	450	89.447	2.234	-16.238	0.9977
	350	3207.537	8.1381	-25.955	0.9960
Ca-Bentonite 1:1 UE	400	231.918	3.984	-25.851	0.9973
	450	114.568	2.374	-26.532	0.9984
	350	12890	0.028	-85.340	0.9975
Ca-Bentonite 2:1 MS	400	1549.378	1.818×10^{-5}	-54.394	0.9965
	450	542.590	2.99×10^{-6}	-41.960	0.9946
	350	8784.110	0.037	-65.092	0.9982
Ca-Bentonite 2:1 UE	400	1075.256	7.904×10^{-5}	-46.198	0.9985
	450	666.017	1.171×10^{-6}	-50.314	0.9956

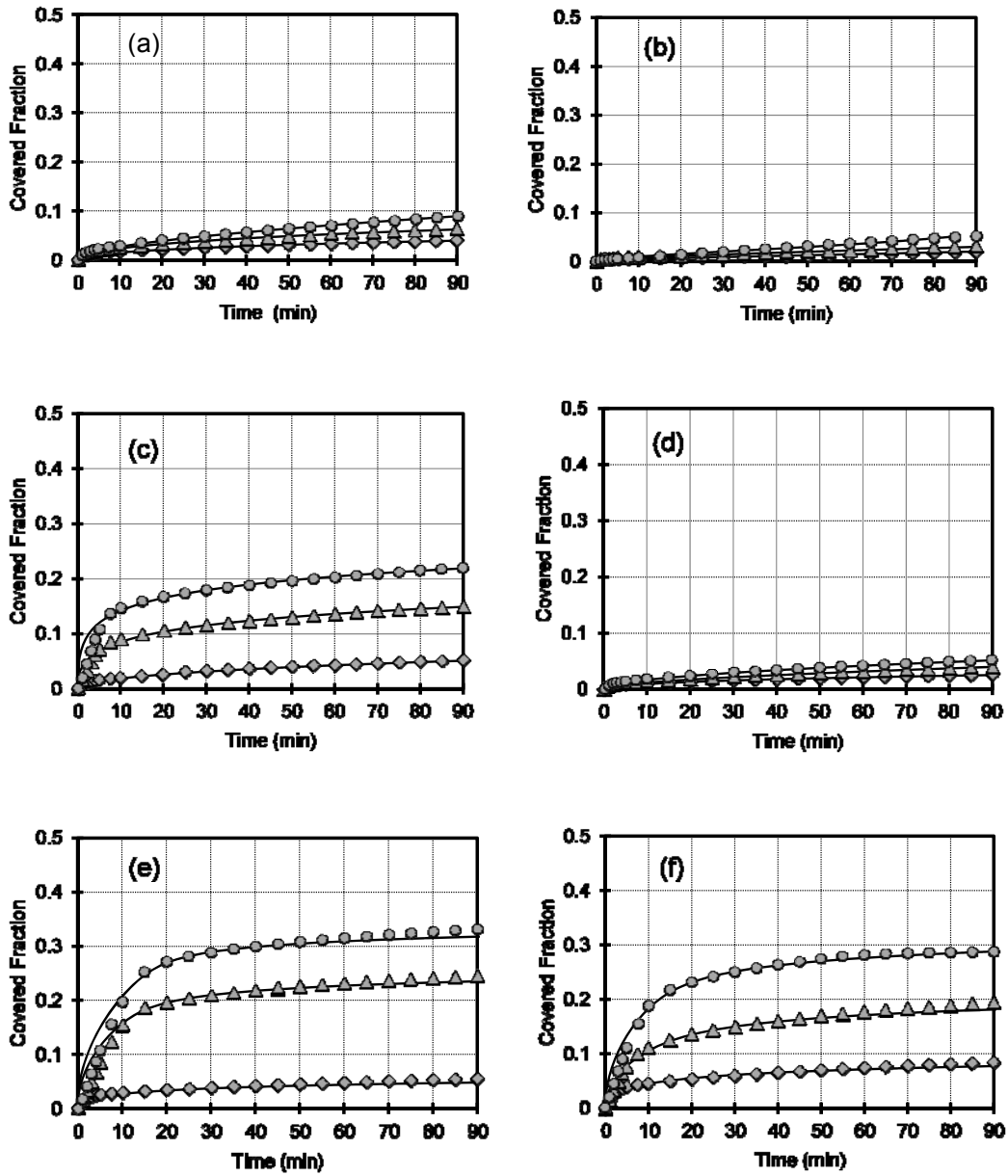
217
218
219
220
221
222

To determine the dependency of the diffusion coefficient, D_{e0} , with respect to temperature, it is necessary to point out that it cannot be directly determined because ρ_B and R , which are other physical parameters involved in k , were not experimentally determined. However, some trends with respect to temperature, support, and preparation method are detected. First, it is critically important to emphasize that if the numerical value of k decreases, it

223 implies that D_{e0} increases since the other parameters are constant, and vice versa, an
 224 increase of k means a reduction in the diffusion coefficient. It is observed that in all the
 225 prepared materials (regardless the support, Ca load, or preparation method) as temperature
 226 increases the value of D_{e0} also raises. So, an Arrhenius-type dependence with respect to
 227 temperature can be obtained. Activation energy was calculated and is presented in Tables 4
 228 and 5. In some cases, confidence limits are quiet high, but they are still statistically
 229 acceptable. These variations may be attributed to the Ca species that are formed during the
 230 reaction. At low Ca loads the activation energy of material supported on tonsil is smaller
 231 compared to those supported on bentonite; however, when increasing the Ca load, the
 232 activation energy of material supported on bentonite is less when ultrasonic energy is
 233 applied during preparation method. This confirms the previous statement that materials
 234 supported on bentonite give better results as the Ca load and temperature augments.
 235



237 **Fig. 5. Adjustment of the experimental data to the kinetics proposed model for**
238 **Ca(OH)₂ supported on bentonite: ◆ 350°C, ▲ 400°C, ● 450°C. (a) MS 1:2; (b) UE 1:2; (c)**
239 **MS 1:1; (d) UE 1:1; (e) MS 2:1; (f) UE 2:1**
240
241
242
243
244
245
246
247
248
249
250



251
 252
 253
 254
 255
 256
 257
 258
 259
 260
 261
 262

Fig. 6. Adjustment of the experimental data to the kinetics proposed model for Ca(OH)_2 supported on tonsil: \blacklozenge 350°C, \blacktriangle 400°C, \bullet 450°C. (a) MS 1:2; (b) UE 1:2; (c) MS 1:1; (d) UE 1:1; (e) MS 2:1; (f) UE 2:1

263
264
265
266
267

Table 4. Activation energy for the SO₂ sorption process in materials supported on tonsil.

Material	E _A /R [K ⁻¹]
Ca-Tonsil 1:2 MS	7,789.5 ± 492.31
Ca-Tonsil 1:2 UE	10,070.0 ± 8,203.81
Ca-Tonsil 1:1 MS	18,410.0 ± 7,004.00
Ca-Tonsil 1:1 UE	4,710.2 ± 2,847.00
Ca-Tonsil 2:1 MS	15,830.0 ± 6,998.00
Ca-Tonsil 2:1 UE	10,590.0 ± 26.07

268
269
270
271
272

Table 5. Activation energy for the SO₂ sorption process in materials supported on bentonite.

Material	E _A /R [K ⁻¹]
Ca-Bentonite 1:2 MS	8,656.7 ± 1,705.43
Ca-Bentonite 1:2 UE	10,940.0 ± 5,493.74
Ca-Bentonite 1:1 MS	14,130.0 ± 5,190.00
Ca-Bentonite 1:1 UE	15,200.0 ± 5,525.00
Ca-Bentonite 2:1 MS	14,370.0 ± 2,752.00
Ca-Bentonite 2:1 UE	11,780.0 ± 4,718.00

273
274
275
276

4. CONCLUSION

277
278
279
280
281
282
283
284
285
286
287
288
289
290
291
292
293
294
295
296
297
298

Materials based on Ca(OH)₂ and supported on bentonite and tonsil were prepared at different mass ratios and tested in a thermogravimetric balance to determine their SO₂ sorption capacity. These materials were active for the desulfurization of flue gases, and their activity was improved as the calcium load and temperature increased. On the other hand, support was not important since the activity was almost the same at different experimental conditions; however, at low temperature activity was slightly better for materials supported on tonsil, but those supported on bentonite gave better results as the Ca load and temperature increased. When ultrasonic energy was applied during the preparation of the sorbent materials, their activity decreased, and it was attributed to an agglomeration of Ca particles, so the available active sites decreased. The SO₂ sorption process was represented by a modified shrinking core process model, and the kinetics parameters were estimated using PolymathTM. It was found that the effective diffusion coefficient increased with temperature. Activation energy of materials supported on bentonite was greater at low Ca load, but as this load increased, their activation energy was smaller compared to materials supported on tonsil.

ACKNOWLEDGEMENTS

The authors acknowledge to CONACYT the financial support through the project 61572.

299
300
301
302
303
304
305
306
307
308
309
310
311
312
313
314
315
316
317
318
319
320
321
322
323
324
325
326
327
328
329
330
331
332
333
334
335
336
337
338
339
340
341
342
343
344
345
346
347
348
349
350

REFERENCES

1. Barreca, A. I., Neidell, M. and Sanders, N. J. (2017). Long-Run Pollution Exposure and Adult Mortality: Evidence from the Acid Rain Program (No. w23524). National Bureau of Economic Research.
2. Di Maria, C., Lange, I. and Van der Werf, E. (2014). Should we be worried about the green paradox? Announcement effects of the Acid Rain Program. *Eur. Econ. Rev.*, 69, 143-162.
3. Burns, D. A., Aherne, J., Gay, D. A., and Lehmann, C. (2016). Acid rain and its environmental effects: Recent scientific advances. *Atmos. Environ.*, 146, 1-4.
4. Chanel, O., Henschel, S., Goodman, P. G., Analitis, A., Atkinson, R. W., Le Tertre, and Medina, S. (2014). Economic valuation of the mortality benefits of a regulation on SO₂ in 20 European cities. *Eur. J. Public Health*, 24(4), 631-637.
5. Raymond, B. A.; Basingthwaite, T.; D. P. (2010). Measuring nitrogen and sulphur deposition in the Georgia Basin, British Columbia, using lichens and moss, *J. Limnol.*, 69, 22-32.
6. Rosi-Marshall, E. J., Bernhardt, E. S., Buso, D. C., Driscoll, C. T., and Likens, G. E. (2016). Acid rain mitigation experiment shifts a forested watershed from a net sink to a net source of nitrogen. *Proceedings of the National Academy of Sciences*, 113(27), 7580-7583.
7. Aksoyoglu, S., Keller, J., Ciarelli, G., Prévôt, A. S. H., and Baltensperger, U. (2014). A model study on changes of European and Swiss particulate matter, ozone and nitrogen deposition between 1990 and 2020 due to the revised Gothenburg protocol. *Atmos. Chem. Phys.*, 14(23), 13081-13095.
8. Bento, A., Freedman, M., and Lang, C. (2015). Who benefits from environmental regulation? Evidence from the clean air act amendments. *Rev. Econ. Stat.*, 97(3), 610-622.
9. Chestnut, L.G.; Mills, D. M. (2005). A fresh look at the benefits and costs of the US acid rain program, *J. Environ. Manage.*, 77, 252-266.
10. Ferris, A. E., Shadbegian, R. J., and Wolverton, A. (2014). The effect of environmental regulation on power sector employment: Phase I of the Title IV SO₂ trading program. *J. Assoc. Environ. Resour. Econ.*, 1(4), 521-553.
11. Cheng, J.; Zhou, J.; Liu, J.; Zhou, Z.; Huang, Z.; Cao, X.; Zhao, X.; Cen, K. (2003). Sulfur removal at high temperature during coal combustion in furnaces: A review, *Prog. Energy Combust. Sci.*, 29, 381-405.
12. Du, Y. J., Wei, M. L., Reddy, K. R., Liu, Z. P., and Jin, F. (2014). Effect of acid rain pH on leaching behavior of cement stabilized lead-contaminated soil. *J. Hazard. Mater.*, 271, 131-140.
13. Srivastava, R.K., Miller, C.A., Erickson, C., and Jambhekar, (2004). R. Emissions of sulfur trioxide from coal-fires power plants, *J. Air Waste Manage. Assoc.*, 54, 750-762.
14. Chen, H., and Khalili, N. (2017). Fly-Ash-Modified Calcium-Based Sorbents Tailored to CO₂ Capture. *Ind. Eng. Chem. Res.*, 56(7), 1888-1894.
15. Donat, F., and Müller, C. R. (2018). A critical assessment of the testing conditions of CaO-based CO₂ sorbents. *Chem. Eng. J.*, 336, 544-549.
16. Gong, G.; Ye, S.; Tian, Y.; Cui, Y.; Chen, Y. (2008). Characterization of blast furnace slag-Ca(OH)₂ sorbents for flue gas desulfurization, *Ind. Eng. Chem. Res.*, 47, 7897-7902.
17. He, D., Shao, Y., Qin, C., Pu, G., Ran, J., and Zhang, L. (2016). Understanding the Sulfation Pattern of CaO-Based Sorbents in a Novel Process for Sequential CO₂ and SO₂ Capture. *Ind. Eng. Chem. Res.*, 55(39), 10251-10262.
18. Karatepe, N.; Erdogan, N.; Ersoy-Mericboyu, A.; Kucukbayrak, S. (2004). Preparation of diatomite/Ca(OH)₂ sorbents and modelling their sulphation reaction, *Chem. Eng. Sci.*, 59, 3883-3889.

- 351 19. Li, T.; Zhuo, Y.; Lei, J.; Xu, X. (2007). Simultaneous removal of SO₂ and NO by low cost
352 sorbent-catalysts prepared by lime, fly ash and industrial waste materials, *Korean J.*
353 *Chem. Eng.*, 24, 1113-1117.
- 354 20. Macias-Perez, M. C.; Bueno-Lopez, A.; Lillo-Rodenas, M. A.; Salinas-Martinez de Lecea,
355 C.; Linares-Solano, A. (2007). SO₂ retention on CaO/activated carbon sorbents. Part I:
356 Importance of calcium loading and dispersion, *Fuel*, 86, 677–683.
- 357 21. Renedo, M. J., Gonzalez, F.; Pesquera, C.; Fernandez, J. (2006). Study of sorbents
358 prepared from clays and CaO or Ca(OH)₂ for SO₂ removal at low temperature, *Ind. Eng.*
359 *Chem. Res.*, 45, 3752-3757.
- 360 22. Bartos, C., Kukovecz, Á., Ambrus, R., Farkas, G., Radacsi, N., and Szabó-Révész, P.
361 (2015). Comparison of static and dynamic sonication as process intensification for
362 particle size reduction using a factorial design. *Chem. Eng. Process. Process Intensif.*,
363 87, 26-34.
- 364 23. Bukhari, S. S., Behin, J., Kazemian, H., and Rohani, S. (2015). Conversion of coal fly
365 ash to zeolite utilizing microwave and ultrasound energies: a review. *Fuel*, 140, 250-266.
- 366 24. Kotadia, H. R., and Das, A. (2015). Modification of solidification microstructure in hypo-
367 and hyper-eutectic Al–Si alloys under high-intensity ultrasonic irradiation. *J. Alloys*
368 *Compd.*, 620, 1-4.
- 369 25. Lim, W. T. L.; Zhong, Z.; Borgna, A. (2009). An effective sonication-assisted reduction
370 approach to synthesize highlydispersed Co nanoparticles on SiO₂, *Chem. Phys. Lett.*,
371 471, 122-127.
- 372 26. Poli, A. L.; Batista, T.; Schmitt, C. C.; Gessner, F.; Neumann, M. G. (2008). Effect of
373 sonication on the particle size of montmorillonite clays, *J. Colloid. Interface Sci.*, 325,
374 386-390.
- 375 27. Lin, R. B., Shih, S. M., and Liu, C. F. (2003). Structural properties and reactivities of
376 Ca(OH)₂/fly ash sorbents for flue gas desulfurization, *Ind. Eng. Chem. Res.*, 42, 1350-
377 1356.
- 378 28. Bahrin, D., Subagjo, S., and Susanto, H. (2016). Kinetic study on the SO₂ adsorption
379 using CuO/γ-Al₂O₃ adsorbent. *Bull. Chem. React. Eng. Catal.*, 11(1), 93-99.
- 380 29. Lee, K. T., and Koon, O. W. (2009). Modified shrinking unreacted-core model for the
381 reaction between sulfur dioxide and coal fly ash/CaO/CaSO₄ sorbent, *Chem. Eng. J.*,
382 146, 57–62.
- 383 30. Lv, L., Yang, J., Shen, Z., Zhou, Y., & Lu, J. (2017). Effect of additives on limestone
384 reactivity in flue gas desulfurization. *Energy Sources Part A*, 39(2), 166-171.
- 385 31. Renedo, M. J., and Fernandez, J. (2004). Kinetic modelling of the hydrothermal reaction
386 of fly ash, Ca(OH)₂ and CaSO₄ in the preparation of desulfurant sorbents. *Fuel*, 83(4-5),
387 525-532.
- 388 32. Wang, J., Guo, J., Parnas, R., and Liang, B. (2015). Calcium-based regenerable
389 sorbents for high temperature H₂S removal. *Fuel*, 154, 17-23.
- 390 33. Yang, Q., and Lin, Y.S. (2006). Kinetics of carbon dioxide sorption on perovskite-type
391 metal oxides. *Ind. Eng. Chem. Res.*, 45, 6302-6310.
- 392 34. Zhao, R., Liu, H., Ye, S., Xie, Y., and Chen, Y. (2006). Ca-based sorbents modified with
393 humic acid for flue gas desulfurization, *Ind. Eng. Chem. Res.*, 45, 7120-7125.

394
395
396
397